Bioorganic & Medicinal Chemistry 16 (2008) 7107–7116

Contents lists available at ScienceDirect

Bioorganic & Medicinal Chemistry

journal homepage: www.elsevier.com/locate/bmc

Sulfur-substituted naphthalimides as photoactivatable anticancer agents: DNA interaction, fluorescence imaging, and phototoxic effects in cultured tumor cells

Ingo Ott [a,b,*], Yufang Xu [a], Jianwen Liu [a], Malte Kokoschka [c], Melanie Harlos [c], William S. Sheldrick [c], Xuhong Qian [a,*]

[a] State Key Laboratory of Bioreactor Engineering and Shanghai Key Laboratory of Chemical Biology, East China University of Science and Technology, Meilong Road 130, Shanghai 200237, China
[b] Institute of Pharmacy, Freie Universität Berlin, Königin-Luise-Str. 2+4, 14195 Berlin, Germany
[c] Lehrstuhl für Analytische Chemie, Ruhr-Universität Bochum, 44780 Bochum, Germany

ARTICLE INFO

Article history:
Received 20 May 2008
Revised 26 June 2008
Accepted 27 June 2008
Available online 2 July 2008

Keywords:
Antitumor drugs
Naphthalimides
Phototoxicity
Photodynamic therapy
Photoinduced electron transfer (PET)

ABSTRACT

A series of sulfur-substituted naphthalimides (**1–5**) was prepared and investigated as antitumor drugs. Initial DNA interaction studies (by the fluorescence quenching method, UV/vis and CD spectroscopy, thermal denaturation, topoisomerase Western blot analysis, and DNA photocleavage experiments) expectedly suggested the DNA and topoisomerase as main targets of the agents. Fluorescence spectroscopic and microscopic experiments indicated a significant sensitivity of the emission intensities of **3** and **5** to the cellular environment and confirmed the cellular uptake and biodistribution into cell compartments for **1–3** and **5**. A comparative evaluation of the antiproliferative effects under different experimental setups (concerning drug exposure period and an additional short-time UV irradiation) revealed significant phototoxic effects for the environmentally sensitive compounds **3** and **5** and strongly suggested the further development of sulfur-substituted naphthalimides for potential use in photodynamic tumor therapy.

1. Introduction

Despite tremendous efforts in the development of new drugs and therapeutic procedures cancerous diseases are still difficult to treat and the development of effective anticancer medicines remains one of the main goals of modern medicinal chemistry research. As cancer cells are highly proliferative tissues, one of the most promising biological targets to decrease tumor cell growth is the DNA.

Among the agents directly interacting with the DNA naphthalimide derivatives have gained considerable attention based on their DNA-intercalating properties and topoisomerase-poisoning activities. The first drugs of this group that reached the clinical trial stage were amonafide and mitonafide (see Fig. 1). However, due to unexpected central neurotoxicity and limited efficiency, the clinical studies on these two drugs met some problems.

Amonafide has so far failed to enter clinical phase III and has long been challenged by its unpredictable side effects (e.g., dose-limiting bone marrow toxicity). In clinic, it was found that amonafide was easily metabolized to *N*-acetyl-amonafide via N-acetylation of the 5′-primary-amino group on the aromatic ring by *N*-acetyltransferase 2, which caused a high-variable, unpredictable toxicity because of the interindividual differences in N-acetylation and greatly obstructed its clinical development. Challenged by such a toxic issue and for avoiding the release of N-acetylated metabolites a broad variety of novel compounds (including bisintercalators such as elinafide) has been reported.[1–9]

As the amino group of amonafide undergoes extensive metabolism and the nitro-group of mitonafide was made responsible for toxic side effects, our efforts in the development of novel naphthal-

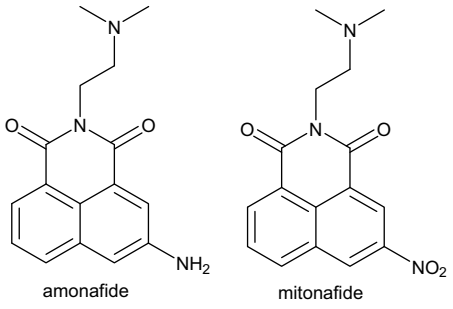

Figure 1. structural formulas of amonafide and mitonafide.

Abbreviations: CD, circular dichroism; PET, photoinduced electron transfer.

* Corresponding authors. Tel.: +86 21 64253589; fax: +86 21 65252603.
E-mail addresses: ottingo@zedat.fu-berlin.de (I. Ott), xhqian@ecust.edu.cn (X. Qian).

0968-0896/$ - see front matter © 2008 Elsevier Ltd. All rights reserved.
doi:10.1016/j.bmc.2008.06.052

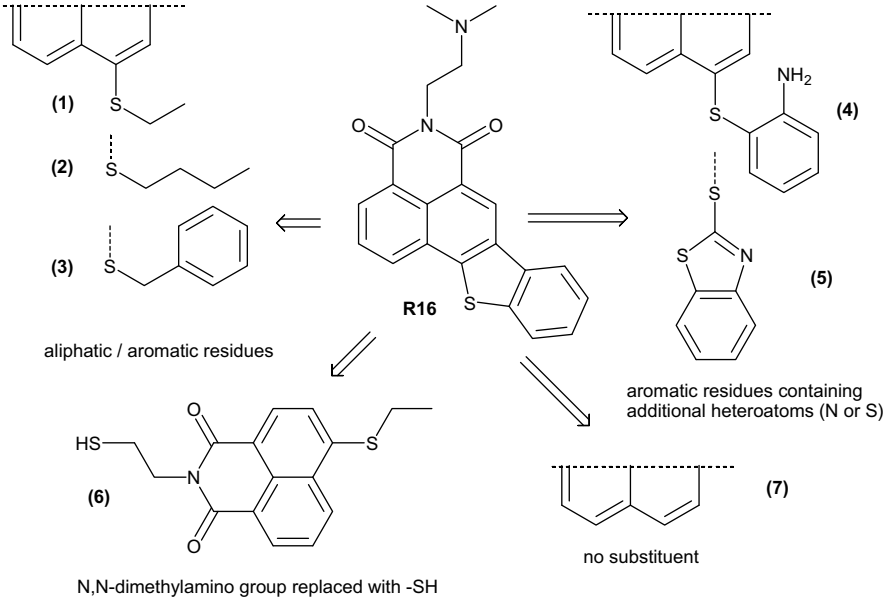

Figure 2. R16, novel target compounds and reference compounds.

imide antitumor drugs have focused so far on tetra- and pentacyclic aromatic derivatives, which lack these supposedly therapeutically problematic functions. This led to the discovery of several naphthalimides containing enlarged fused aromatic ring systems which displayed promising intercalating, DNA photocleaving, and tumor cell growth-inhibiting properties. Among the compounds evaluated so far we noted as an overall result that especially sulfur-containing derivatives showed promising antiproliferative efficiency.[10–12]

One of the most active agents found within our studies is the thio-heterocyclic naphthalimide R16 (see Fig. 2), which exhibited superior cytotoxic effects in comparison to amonafide and mitonafide in several tumor models, acted as a topoisomerase poison and induced apoptosis.[13]

Although many naphthalimides have been prepared and screened for cytotoxic effects, little attention has been paid to simple thio-substituted derivatives and no concrete structure–activity relationship studies involving this substituent have been described so far. Based on the structure of R16 and structurally closely related thio-heterocyclic compounds recently described by Brana et al.,[6] we developed a series of non-ring fused derivatives containing sulfur in position 4 of the naphthalimide ring system (**1**–**5**, see Fig. 2). The target compounds contain the *N*,*N*-dimethylaminoethyl side chain, which is considered to be an optimized pharmacophore concerning the interaction with the DNA backbone and with the topoisomerase enzyme.[1] Compounds, each lacking one of the mentioned properties, were prepared as references (**6** and **7**).

Naphthalimides have also been described as strongly fluorescent agents[14–15] and photoactivatable species that exhibit significant DNA photocleaving[10,11,16–20] activities. Interestingly, to the best of our knowledge these properties have not been used so far to evaluate the compounds as phototoxic antitumor drugs in vitro or in vivo although there are few reports on the use as photoactivatable antiviral agents.[21–22] However, the presence of phototoxic properties might widen the applicability of this class of cytostatics concerning the use in photodynamic therapy.[23] The investigation of sulfur-substituted naphthalimides appears very promising in this context based on recent observations showing that the DNA photocleaving potency of thio or thiono naphthalimides was significantly higher than that of the corresponding oxygen derivatives.[24]

This report deals with the preparation and basic fluorescence characteristics of a series of novel thiosubstituted naphthalimides, the study of their DNA interaction properties, cellular uptake and intracellular distribution by fluorescence microscopy as well as the in-vitro evaluation of their phototoxicity.

2. Results

2.1. Synthesis and fluorescence spectra

The synthesis of the target compounds was performed according to established procedures as depicted in Scheme 1.[10,12,16–19] Commercially available 4-bromo-1,8-naphthalic anhydride was reacted with the thiols to the corresponding 1,8-naphthalic anhydride thioethers, which were then transformed into the target compounds by refluxing with *N*,*N*-dimethlyaminoethylamine or cysteamine in absolute ethanol. All target compounds used for the biochemical assays were purified by column chromatography over SiO_2 and structurally confirmed by ^1H NMR, MS, and elemental analyses.

Fluorescence spectra were recorded in phosphate-buffered saline solution, pH 7.4 (PBS) under experimental conditions that were also used for the study of the DNA binding by the fluorescence-quenching method (see below).

The unsubstituted reference compound **7** showed an intense maximum around E_x/E_m 344/396 nm. For the ethyl-, butyl-, and benzyl-substituted derivatives **1–3**, this maximum was shifted toward longer wavelengths (E_x/E_m 396–403/506–523 nm; see Fig. 3 for representative examples) but no significant fluorescence intensity was observed with the derivatives **4** and **5** containing additional heteroatoms (N and S) on the sulfur substituent. Absolute fluorescence intensities at the respective E_x/E_m maxima of 5 μM of the compounds in PBS increased in the series **3** (649) < **7** (1896) < **1** (2968) < **2** (3539).

The weak or missing fluorescence emission of **3–5** can be attributed to changes in the photoinduced intramolecular electron transfer (PET) caused by the aromatic substituents on the sulfur. PET between the electron rich amino moiety and the relatively electron-deficient naphthalimide fluorophore component can be expected to be significantly influenced by these aromatic/heteroaromatic moieties.[25–27]

2.2. Interaction with the DNA

Based on their fluorescence-emitting properties, we studied the binding of **1–3** and **7** to DNA by the fluorescence-quenching meth-

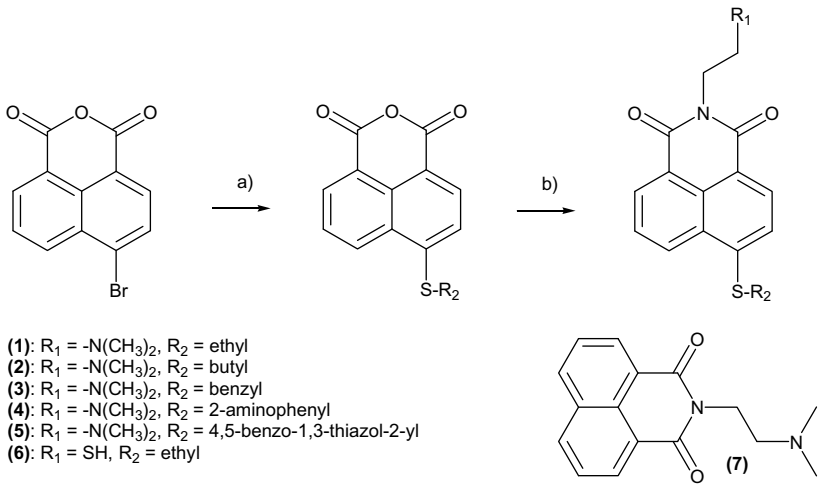

Scheme 1. Synthesis of the target compounds. Reagents conditions: (a) thiol (R_2-SH), DMF, K_2CO_3, 30–50 °C, 3–7 h; (b) *N*,*N*-dimethylethylamine or cysteamine, EtOH (abs), reflux 5–7 h.

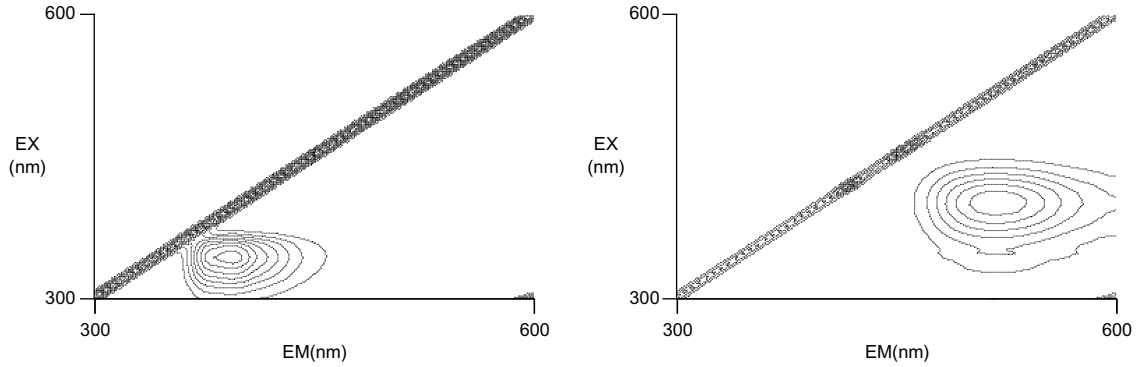

Figure 3. Contour plots of 3D fluorescence scans of 5.0 μM of 7 (left) and 1 (right) in phosphate-buffered saline pH 7.4.

od. Figure 4 (top) shows exemplarily the quenching of the emission curve of 5.0 μM of **1** by increasing (5–400 μM) amounts of DNA. In Figure 4 (bottom), the relative fluorescence intensities at the maxima of **1–3** and **7** are plotted against the concentration of DNA.

Emissions for the stronger fluorescent target compounds **1** and **2** decreased exponentially and reached values under 50% of the initial fluorescence at incubation with 400 μM DNA. In contrast to this, the emission of **3** could not be influenced strongly by the presence of DNA (>80% relative intensity at all concentrations) and for **7** the decrease in emission followed an almost linear trend. However, for all compounds fluorescence-quenching at least at the highest DNA concentration (400 μM) could be observed, which is in good agreement with a broad series of previous studies by different groups suggesting naphthalimides as agents with intercalating properties.[1,7,8,10,12,17]

UV/vis spectroscopy, CD (circular dichroism) spectroscopy, and thermal denaturation studies offer useful tools to study the DNA interaction independent of the presence of fluorescence properties.[28]

The UV/vis spectra of **1**–**7** incubated with DNA at $r = 0.1$ (r = [compound]/[DNA]) for 60 min showed bathochromic and hypochromic shifts in the case of **1**, **2**, **4**, **5**, and **7** (see Fig. 5 and SI). For **3** a significant bathochromic and a slight hyperchromic shift could be noted. This pattern could be caused by intramolecular π–π interactions between the aromatic ring of the side chain and the naphthalimide core, which counteract an intercalative interaction with the DNA.

The spectra recorded with **6** showed no bathochromic shift. However, a slight hyperchromic shift was observed for this compound.

In general, these results indicated intercalative properties for **1**–**5** and **7** but not for **6**. This can be attributed to the absence of the nitrogen in the side chain of **6**, which reduced the ability of the compound to interact with the DNA (the protonable nitrogen in the side chain is required to enable an initial electrostatic contact with the negatively charged DNA phosphate backbone prior to intercalation between the bases). It should be noted that in the case of **5** a broadening of the absorption maximum was observed (see Fig. 5, right), which indicates significant changes in the electron distribution upon interaction with the nucleobases.

Changes in the DNA melting temperature upon interaction with an intercalating compound provide an effective means to estimate the efficacy of intercalation. Melting temperature shifts ΔT_m for **1**–**7** are listed in Table 1. For **1**–**4** and **7** values between 6 and 9 °C were measured and are indicative of an intercalative mode of interaction with the DNA. Small ΔT_m values were found for **5** and **6** correlating to low intercalative efficacy.

Circular dichroism (CD) spectroscopy can be used to monitor conformational changes of the DNA biopolymer as a consequence of interaction with drugs. The CD spectrum of DNA shows a negative peak at approximately 245 nm caused by the helical B conformation and a positive peak at approximately 275 nm due to base stacking.

Incubation of DNA with **1**–**3** (see Fig. 6, left) led to a decrease of the negative peak and an increase of the positive peak. Both effects

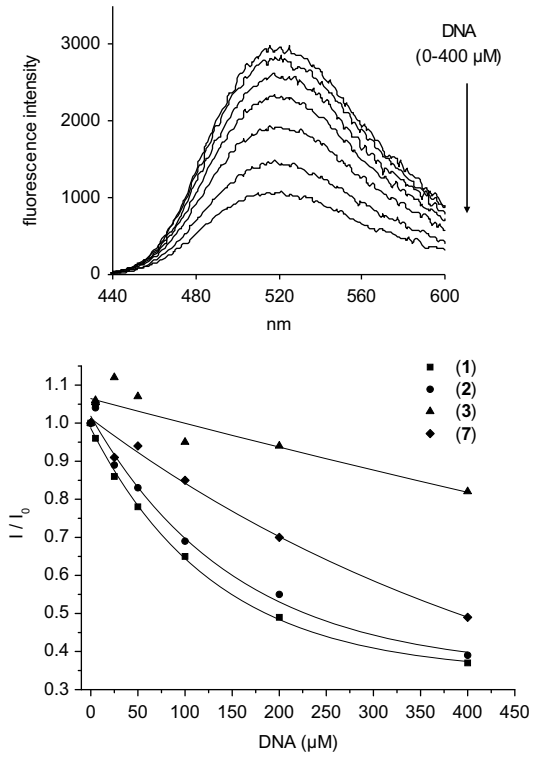

Figure 4. Top: Quenching of the fluorescence emission curve of 5.0 μM of 1 by increasing concentrations of DNA (37 °C, 1 h); bottom: fluorescence quenching of the maxima of 5 μM of **1**–**3** and **7** by increasing concentrations of DNA (37 °C, 1 h); emissions were recorded at the respective E_x/E_m maxima (E_x/E_m **1**, 402/521; **2**, 403/519; **3**, 396/511; **7**, 344/396 nm), I: fluorescence intensity in the presence of DNA, I0: fluorescence intensity in the absence of DNA

Table 1
Melting temperature shifts ΔT_m [°C] for the interaction of **1**–**7** with DNA at r = [compound]/[DNA] = 0.1

Compound	ΔT_m (°C)
1	8
2	8
3	7
4	9
5	3
6	2
7	6

are in agreement with intercalative properties of the compounds. For **4** a strong decrease and deformation of the negative peak but no significant change of the positive peak was observed. This pattern could be the consequence of a –NH. . .O hydrogen-bonding interaction between the aniline nitrogen of **4** and a carbonyl group of the nucleobases. Similar to the results obtained with **1**–**3** compounds **5** and **7** showed a decrease of the negative peak and an enhancement of the positive peak (most marked for **7**). No significant changes were noted for **6**, which is in good agreement with the above-described results concerning UV/vis spectroscopy and thermal denaturation.

As there are several reports on DNA photodamage and photocleaving mechanisms of naphthalimides, we investigated if the target compounds **1–5** were able to photocleave pBR322 plasmid DNA under UV irradiation conditions. Compounds **6** and **7** were used as references. In this assay, the photocleaving efficacies of **3** and **5** were slightly more pronounced than those of **1**, **2**, **4**, **6**, and **7** (see Fig. 7). This indicates that sulfur-substituted naphthalimides could be suitable for triggering phototoxic effects, which is in line with a series of previous findings.[10,16–19]

Besides DNA intercalation and photocleavage, the interaction with the topoisomerase system has been made responsible for the antiproliferative effects triggered by naphthalimides such as R16.[1,13]. Accordingly, the influence of **1**–**5**, **7** and R16 on topoisomerase IIα (Topo IIα) was evaluated by Western blot analysis (see Fig. 8). This assay does not enable to determine an inhibitory effect of the target compounds on topoisomerase but it reflects changes in the expression of the enzyme, which may be the consequence of a direct or indirect intracellular interaction with the enzyme itself or with related biochemical pathways.

In this assay **1, 4**, and **5** and both reference compounds strongly reduced Topo IIα protein levels, **2** and **3** were devoid of activity. As the non-sulfur compound **7** displayed almost the same activity as **1, 4, 5**, and R16, it can be concluded that the effect was independent of the presence of the sulfur substituent on position 4 of the ring system. The inactivity of **2** and **3** in this assay indicated that long lipophilic side chains are not well tolerated.

2.3. Fluorescence-imaging: cellular uptake, intracellular distribution, and photobleaching

The target compounds seemed suitable for fluorescence microscopic studies concerning their cellular uptake and biodistribution into the nuclei of tumor cells. For this purpose, MCF-7 human breast cancer cells were selected, incubated with the drugs, and investigated using a fluorescence microscope equipped with a E_x/E_m $390^{\pm11}/460^{\pm25}$ nm filter.

As expected, due to the fluorescence characteristics described above, the cellular uptake of **1** and **2** was confirmed clearly by the significant blue emission of the compounds (see Fig. 9). In contrast to this **4** and **7** could not be visualized, which can be attributed on the one hand to the weak intrinsic fluorescence noted for **4** and on the other hand to the E_x/E_m 344/396 maximum of **7**,

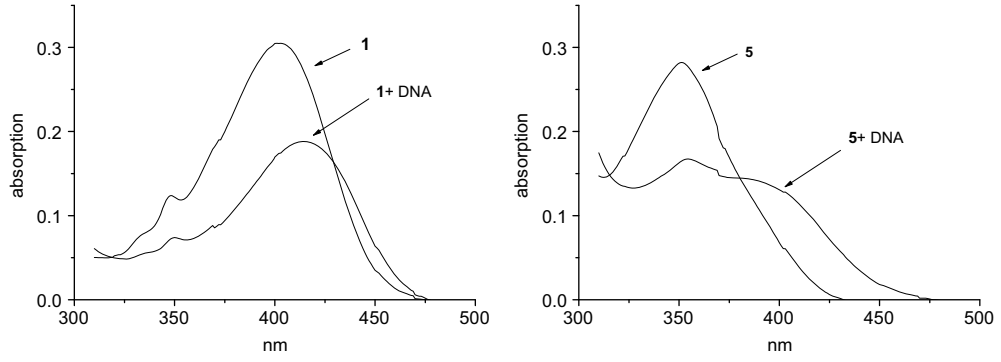

Figure 5. UV/vis spectra of 20 μM of **1** and **5** incubated with DNA (200 μM) for 60 min (corresponding spectra of **2**–**4**, **6**, **7** are available in the SI).

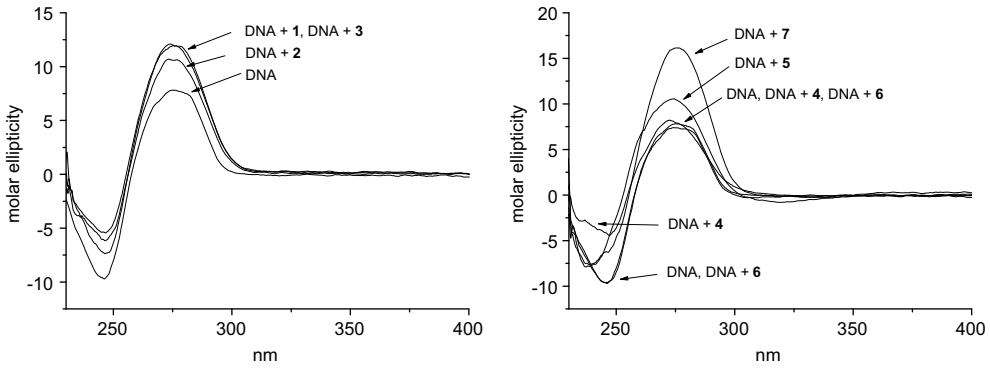

Figure 6. CD spectra of DNA (200 μM) incubated with 20 μM of **1**–**3** (left) and **4**–**7** (right) for 60 min.

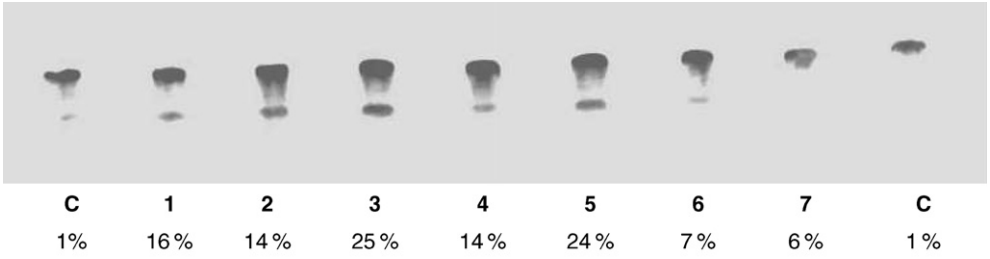

Figure 7. Gel electrophoresis of PBr322 plasmid DNA incubated with 50 μM of **1**–**7** for 2 h under irradiation at 365 nm. Lanes 1 and 9: control (C, no compound), lanes 2–8: compounds **1**–**7**; photocleaving properties are indicated by the appearance of a second DNA band (nicked or linear form) with lower electrophoretic mobility than the control DNA (supercoiled closed circular form). The amount of cleaved DNA is indicated as mean percentage of two independent experiments. (One of the gels is depicted.)

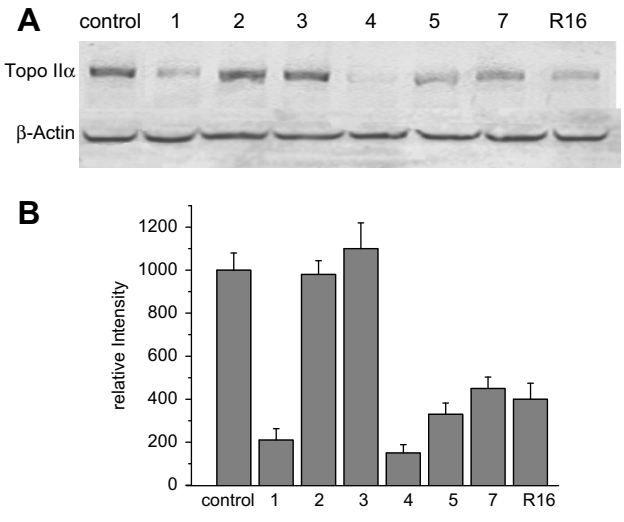

Figure 8. (A) Western blot analysis of protein extracts obtained from HeLa cells treated with drugs at their IC_{50} concentrations (see SI) for 24 h. (B) Quantification of the bands was performed and normalized in relation to untreated cells. β-Actin was used as a loading control. Data are presented as means ± SD of three independent experiments.

which is outside the excitation and emission bandwidths of the used filter.

Unexpectedly, **3** and **5** could be well monitored despite the low or missing fluorescence emission in phosphate-buffered saline pH 7.4 (see Fig. 9, bottom). In fact, there are many reports on the enhancement of naphthalimide fluorescence emission due to the inhibition or switching-off of intramolecular PET processes upon binding to metal ions,[25,28–32] changing the pH value,[14,16,34] or lowering the solvent polarity.[26,34–36] Thus, the fluorescence properties and quantum yields of naphthalimides are largely influenced by their surrounding chemical environment and binding to membranes or biological macromolecules as well as different pH values within the cell will strongly affect the fluorescence properties of the compounds.

As shown in Figure 9 the fluorescence intensity appeared to be spread all over the cells but more intensive spots indicated an accumulation of the target compounds in cell compartments such as the nucleus (this effect was most marked for **5**).

During microscopy photobleaching (decrease of emission intensity) was noted leading to an almost complete loss of blue emission within a 2–4 min irradiation interval (see Fig. 9, middle left).

However, after keeping the cells for 4 min in the dark (no UV irradiation) and repeated irradiation, the blue emission was recovered but it remained stable only for a few seconds. In this case, the blue fluorescence light appeared to be more diffusely spread over the cells and no spots with increased emission intensity were observed. It should be noted that for **5** almost no fluorescence emission was recovered after a 'dark period' whereas for **1** and **3** results comparable with those exemplarily depicted for **2** were obtained (compare Fig. 9 top right and middle pictures).

An important parameter for the fluorescence characteristics of the presented naphthalimides is the protonable nitrogen of the side chain. As shown previously for some structurally closely related compounds, protonation of the nitrogen caused an increase in fluorescence emission.[16] Therefore, we included **6**, in which the *N*,*N*-dimethylamino group is replaced by a mercapto group, in the experiments. In contrast to the well-detectable 1, cells incubated with its thiol derivative **6** did not show any significant blue emission (data not shown).

2.4. Antiproliferative effects and phototoxicity

The antiproliferative effects of **1**–**5** were evaluated in MCF-7 breast cancer and HT-29 colon carcinoma cells. R16, **6**, and **7** were

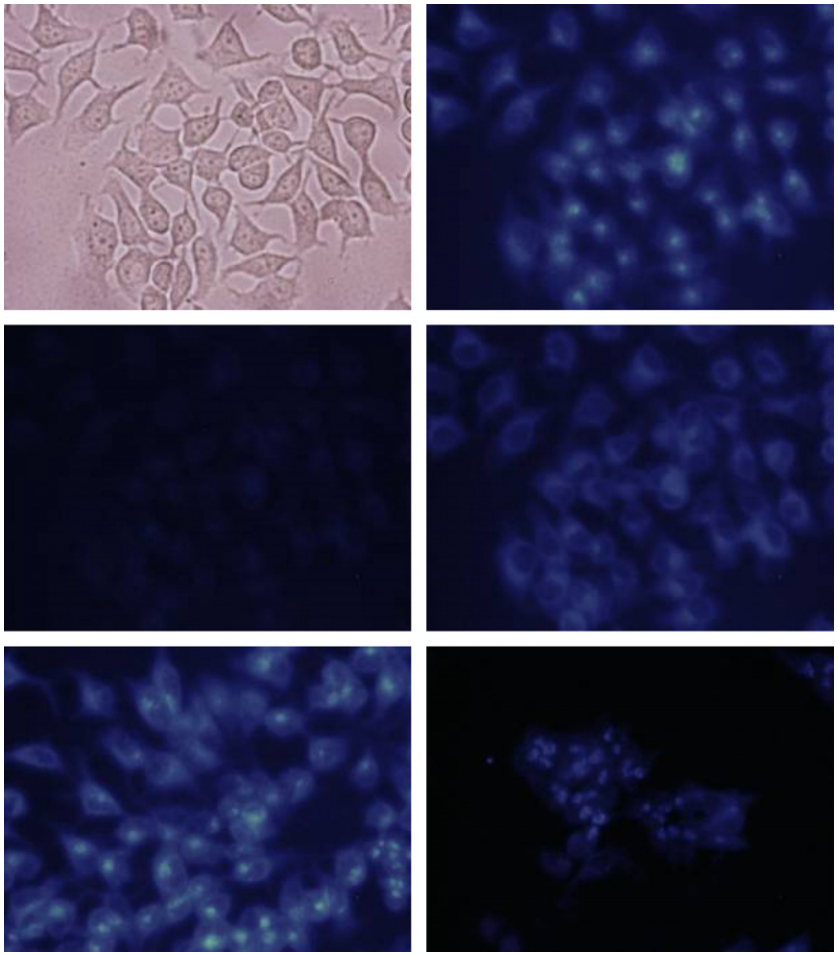

Figure 9. Fluorescence microscopic studies of MCF-7 cells (40-fold enlargement) incubated for 6 h with 10 μM of **2**, **3**, and **5**; top left: cells incubated with **2**, picture taken without using fluorescence equipment; top right: blue emission of **2** after a few seconds of fluorescence microscopy irradiation; middle left: no emission of **2** after 4 min fluorescence microscopy irradiation; middle right: blue emission of **2** after a few seconds of fluorescence microscopy irradiation following a period of 4 min of fluorescence microscopy irradiation and 4 min without irradiation; bottom left: blue emission of **3** after a few seconds of fluorescence microscopy irradiation; bottom right: blue emission of **5** after a few seconds of fluorescence microscopy irradiation.

used as references. Experiments were performed under continuous (72 h for HT-29 and 96 h for MCF-7) exposure to graded concentrations of the compounds or under short-time exposure (24 h) to the drugs followed by additional culture in drug-free media with or without a 20-min 366-nm irradiation interval. According to this experimental setup, only the drug taken up into the cells is irradiated and no toxic photochemical products formed outside the cells will influence the outcome of the results.

In the continuous exposure experiments (see '96 h' and '72 h' columns of Table 2) R16 was with IC_{50} values below 1.0 μM the by far most active compound. However, **1–5** were also highly active and displayed IC_{50} values between 1.9 and 4.6 μM, which are well in the range of established antitumor agents. Thus, cisplatin and 5-fluorouracil showed IC_{50} values of 2.0 and 4.8 μM in the same assay[38] in MCF-7 cells and for amonafide comparable activity in the used cell lines has been reported (IC_{50} value of 1.1 μM in MCF-7 cells[5] and 4.7 μM in HT-29 cells[6,7]). As expected compound **6**, which does not contain the *N*,*N*-dimethylamino pharmacophore required for proper interaction with the DNA or topoisomerase, was devoid of any activity in all the experiments.

Table 2
Antiproliferative effects (IC_{50} value) in MCF-7 and HT-29 cells after continuous exposure to the drugs (MCF-7: 96 h, HT-29: 72 h), short exposure followed by culture in drug-free media (MCF-7: 24/72 h, HT-29: 24/48 h) or short exposure followed by irradiation (20 min, 366 nm) and culture in drug-free media (MCF-7: 24 h/irrad./72 h, HT-29: 24 h/irrad./48 h); experiments were performed in duplicate (each $n = 6$); n.d., not determined

	IC_{50} MCF-7 (μM)			IC_{50} HT-29 (μM)		
	96 h	24/72 h	24 h/irrad./72 h	72 h	24/48 h	24 h/irrad./48 h
1	$4.4^{\pm1.6}$	$4.5^{\pm0.7}$	$4.3^{\pm0.5}$	$1.9^{\pm0.1}$	$2.2^{\pm0.3}$	$2.5^{\pm0.4}$
2	$2.6^{\pm0.6}$	$5.7^{\pm1.0}$	$4.0^{\pm0.3}$	$4.6^{\pm0.2}$	$4.3^{\pm0.0}$	$3.0^{\pm0.5}$
3	$3.4^{\pm0.5}$	$6.7^{\pm1.1}$	$1.7^{\pm0.4}$	$4.1^{\pm0.1}$	$4.8^{\pm0.4}$	$1.3^{\pm0.0}$
4	$2.6^{\pm0.9}$	$4.8^{\pm1.6}$	$4.9^{\pm1.8}$	$2.9^{\pm0.9}$	$2.8^{\pm0.7}$	$2.8^{\pm0.3}$
5	$2.7^{\pm0.5}$	$7.3^{\pm0.4}$	$2.4^{\pm0.6}$	$4.4^{\pm1.4}$	$5.5^{\pm1.1}$	$1.8^{\pm0.4}$
6	>50	>50	>50	n.d.	>50	>50
7	$4.5^{\pm0.3}$	$11.6^{\pm3.8}$	$11.3^{\pm3.3}$	$3.5^{\pm0.9}$	$7.2^{\pm0.8}$	$5.3^{\pm0.3}$
R16	$0.20^{\pm0.03}$	$0.17^{\pm0.01}$	$0.18^{\pm0.02}$	$0.62^{\pm0.18}$	$0.23^{\pm0.03}$	$0.21^{\pm0.06}$

Interestingly, in the continuous exposure experiments no significant effect of the sulfur substituents of **1–5** could be noted as the unsubstituted counterpart **7** exhibited comparable activity. This result was surprising as the ring-fused thio-heterocyclic R16 was the most active substance in the studied series.

Short time exposure (24 h) to the agents followed by incubation in drug-free media showed in most of the experiments an increase of the IC_{50} values in MCF-7 cells but in HT-29 cells no strong effect could be noted (compare '24 h/72 h' and '24 h/48 h' columns in Table 2 with the corresponding '96 h' and '72 h' columns). This is most probably the consequence of the longer incubation period used for MCF-7 cells (which is based on the slower growth characteristics of MCF-7 cells compared to HT-29 cells, see SI) allowing a more effective recovery from the initial drug exposure period.

Analogous experiments including a 20 min irradiation interval at 366 nm showed 3–5 times decreased IC_{50} values for **3** and **5** in both investigated cell lines (for MCF-7 cells compare the '24 h/72 h' with the '24 h/irrad./72 h' column in Table 2, for HT-29 compare the corresponding '24 h/48 h' and '24 h/irrad./48 h' columns). In contrast to this with **1**, **4**, **6**, and R16 absolutely no changes in the antiproliferative activity could be noted upon irradiation. For **7** in HT-29 and for **2** in both cell lines a very weak (each 1.4-fold lower IC_{50} values) effect of the irradiation procedure was observed.

The enhanced phototoxicity of **3** and **5** might be the consequence of toxic radicals formed during the irradiation period and seems to correlate with the sensitivity of their fluorescence emissions to the surrounding chemical environment (as observed during the microscopy studies) as well as their enhanced photocleaving efficacy (see above).

3. Discussion

A series of sulfur-substituted naphthalimides was prepared and investigated for biological properties. Initial DNA interaction studies (by fluorescence-quenching, UV/vis, thermal denaturation, plasmid DNA photocleaving, and Topo IIα Western blot assays) indicated intercalation into the DNA and interaction with the topoisomerase system as possible modes of drug action of **1**–**5** and **7** and suggested a potential use of the target compounds as photoactivatable antitumor agents. In contrast the reference compound **6**, which does not contain the *N*,*N*-dimethylaminoethyl side chain, was devoid of significant activity in all the mentioned assays.

Fluorescence microscopic studies showed that the compounds were taken up into the cells in significant amounts. Replacement of the *N*,*N*-dimethylamino group with a mercapto group (**6**) prevented fluorescence emission of the cells highlighting the importance of the side chain nitrogen for cellular uptake and/or fluorescence properties. The detectability of **3** and **5**, which exhibited only weak or no fluorescence in buffer solution, was comparable to that of **1** and **2**, which showed strong fluorescence emission in buffer solution. This effect may be attributed to sensitivity of the fluorescence of the compounds to their chemical environment (concerning pH value, polarity, membranes, and macromolecules). Similar properties (meaning weak fluorescence in polar aqueous solvents but intensive fluorescence emission in apolar solvents or upon binding to hydrophobic regions of proteins or membranes) have recently been applied for biological binding studies (e.g., opioide receptor binding) using an environment-sensitive naphthalimide fluorophore.[37,39]

Interestingly, those target compounds (**3** and **5**) that were most susceptible to fluorescence induction in cellular environment and showed enhanced plasmid DNA photocleaving properties triggered significant phototoxic effects in cultured tumor cells (MCF-7 and HT-29) with 3–5 times lowered IC_{50} values after short-time UV irradiation. Although the IC_{50} values of the lead compound R16 could not be reached, the exclusive phototoxicity of **3** and **5** may offer interesting therapeutic advantages concerning the application in photodynamic tumor therapy.

In this context it should be noted that for therapeutic purposes the use of advanced light dosimetry technology (e.g., fibers or inflatable balloons as used for photodynamic treatment of brain tumors[40]) should be envisaged due to the low tissue penetration of low wavelength irradiation.[41] Based on the fact that **3** and **5** displayed antiproliferative effects also under non-irradiation conditions, they could be useful lead compounds for cytostatics that are active under 'normal' therapeutic conditions and can be additionally activated in a controlled manner by the use of advanced optical fiber technology. It can be assumed that under dark conditions intercalation and most probably the interaction with topoisomerase system lead to cell growth-inhibiting effects. Under photoirradiation supposedly the cleavage of DNA contributes additionally to the antiproliferative potency of the agents.

The environmental sensitivity and phototoxic behavior of the presented compounds can be seen as a consequence of the electron distribution over the naphthalimide ring system, which is itself influenced by the residues at the sulfur substituent in position 4. Consequently, changes in electron distribution of the relatively electron-deficient naphthalimide system will affect intramolecular PET processes, which are themselves strongly dependent on the chemical environment.[14,16,25–36]

According to the above-described results the introduction of sulfur substituents containing non fused (hetero)aromatic rings located close to the naphthalimide core can be recommended for further drug development.

4. Conclusion

A series of sulfur-substituted naphthalimides exhibiting the established biological properties of this class of compounds (DNA interaction and antiproliferative effects) was prepared. The present study demonstrates that the development of phototoxic naphthalimides can be realized by introducing appropriate sulfur residues on the 4 position of the naphthalimide core. To the best of our knowledge, this is the first report proving the phototoxicity of naphthalimides in tumor cell culture studies. The fluorescence emission of the target compounds was significantly influenced by the chemical (cellular) environment.

5. Experimental

5.1. General

Chemicals and reagents were purchased from Sigma, Aldrich, and Fluka. PBS: phosphate-buffered saline, pH 7.4; for biochemical assays and in-vitro studies, the compounds were prepared as stock solutions in dimethylsulfoxide (DMSO) and diluted 1:1000 with the respective media. Human-reactive monoclonal antibodies, anti-topoisomerase IIα, were from Thermo Scientific. NMR spectra were recorded on a 400 MHz spectrometer or a 500 MHz NMR spectrometer (Bruker); elemental analysis: Perkin-Elmer 240 C; MS spectra: CH-/A- Varian MAT.

5.2. Cell culture

MCF-7 breast cancer, HT-29 colon carcinoma, and HeLa adenocarcinoma cells were maintained by standard procedures at 37 °C in a humidified atmosphere of 95% air and 5% CO_2; cell culture medium for MCF-7 and HT-29 cells: minimum essential medium eagle supplemented with 2.2 g $NaHCO_3$, 110 mg/L sodium pyruvate, and

50 mg/L gentamicin sulfate and adjusted to pH 7.4. Prior to use 10% (V/V) fetal calf serum was added; cell culture medium for HeLa cells RPMI 1640 medium supplemented with 10% heat-inactivated bovine serum, penicillin (100 U/mL), and streptomycin (100 U/mL).

5.3. Synthesis of sulfur-substituted naphthalic anhydrides

4-Bromo-1,8-naphthalic anhydride (1.75–5.77 mmol) was dissolved in 15 mL dimethylformamide and an excess of thiol and K_2CO_3 were added. After stirring for 3–7 h at ambient temperature (30–50 °C), the suspension was poured into 40 mL distilled water, the precipitate was collected by filtration, washed with distilled water, and dried. In case the ^{1}H NMR spectra showed significant amounts of the mercapto educts, the products were further purified by column chromatography over SiO_2.

5.4. 4-Ethylthio-1,8-naphthalic anhydride

4-Bromo-1,8-naphthalic anhydride: 1.60 g (5.77 mmol); ethanethiol: 0.44 mL (5.99 mmol), K_2CO_3: 0.51 g; 40 °C, 3 h; yield: 1.382 g (93%) yellow crystals; ^{1}H NMR (DMSO-d_6): δ = 1.41 (t, 3H, ^3J = 7.3 Hz, –CH_3), 3.32 (q, 2H, ^3J = 7.3 Hz, –CH_2), 7.78 (d, 1H, ^3J = 7.9 Hz, ArH), 7.92 (ddd, 1H, ^3J = 8.2 Hz, ^3J = 8.3 Hz, ^4J = 0.8 Hz, ArH), 8.40 (d, 1H, ^3J = 7.9 Hz, ArH), 8.57 (m, 2H, 2 ArH).

5.5. 4-Butylthio-1,8-naphthalic anhydride

4-Bromo-1,8-naphthalic anhydride: 485 mg (1.75 mmol), 0.32 mL butane-1-thiol; K_2CO_3: 0.54 g; 30 °C, 7 h; yield: 204 mg (0.71 mmol, 41%) yellow crystals; ^{1}H NMR (DMSO-d_6): δ = 0.94 (t, 3H, ^3J = 7.3 Hz, CH_3), 1.51 (m, 2H, CH_2), 1.74 (m, 2H, CH_2), 3.32 (t, 2H, ^3J = 7.4 Hz, –S–CH_2), 7.80 (d, 1H, ^3J = 7.9 Hz, ArH), 7.92 (m, 1H, ArH), 8.40 (d, 1H, ^3J = 7.9 Hz, ArH), 8.56 (m, 1H, ArH), 8.62 (m, 1H, ArH).

5.6. 4-Benzylthio-1,8-naphthalic anhydride

4-Bromo-1,8-naphthalic anhydride: 703 mg (2.54 mmol), benzylthiol: 0.4 mL, K_2CO_3: 0.55 g; 30–50 °C, 6 h; the crude product was purified by column chromatography over SiO_2 (eluent: $CHCl_3$, $CHCl_3$/MeOH 10:1 and 10:2); yield: 317 mg (0.99 mmol, 39%) yellow crystals; ^{1}H NMR (DMSO-d_6): δ = 4.62 (s, 2H, CH_2), 7.29 (m, 1H, ArH), 7.36 (m, 2H, 2 ArH), 7.52 (m, 2H, 2 ArH), 7.92 (m, 2H, 2 ArH), 8.39 (d, 1H, ^3J = 7.9 Hz, ArH), 8.55 (dd, 1H, ^3J = 7.3 Hz, ^4J = 0.9 Hz), 8.62 (dd, 1H, ^3J = 8.5 Hz, ^4J = 0.9 Hz).

5.7. 4-(2-Aminophenyl)-thio-1,8-naphthalic anhydride

4-Bromo-1,8-naphthalic anhydride: 942 mg (3.40 mmol), *o*-aminothiophenol: 0.4 mL; K_2CO_3: 0.61 g, 40 °C, 6 h; the crude product was purified by column chromatography over SiO_2 (eluent: $CHCl_3$); yield: 687 mg (2.14 mmol, 63%) yellow crystals; ^{1}H NMR (DMSO-d_6): δ = 5.60 (s, 2H, –NH_2), 6.70 (m, 1H, ArH), 6.92 (dd, 1H, ^3J = 8.2 Hz, ^4J = 1.1 Hz, ArH), 7.00 (d, 1H, ^3J = 8.0 Hz, ArH), 7.32 (m, 1H, ArH), 7.40 (dd, 1H, ^3J = 7.7 Hz, ^4J = 1.4 Hz, ArH), 7.99 (m, 1H, ArH), 8.33 (d, 1H, ^3J = 8.0 Hz, ArH), 8.60 (dd, 1H, ^3J = 7.3 Hz, ^4J = 0.8 Hz, ArH), 8.77 (dd, 1H, ^3J = 8.5 Hz, ^4J = 0.8 Hz, ArH), preparation of 4-(2-aminophenyl)-thio-1,8-naphthalic anhydride without structural characterization data has been reported.[19]

5.8. 4-(4,5-Benzo-1,3-thiazol-2-yl)-thio-1,8-naphthalic anhydride

4-Bromo-1,8-naphthalic anhydride: 977 mg (3.53 mmol), 2-mercaptobenzothiazol: 668 mg (3.99 mmol); K_2CO_3: 0.52 g, 45 °C, 7 h; yield: 930 mg (2.56 mmol, 73%) yellow crystals; ^{1}H NMR (DMSO-d_6): δ = 7.39 (m, 1H, ArH), 7.49 (ddd, 1H, ^3J = 8.2 Hz, ^3J = 7.2 Hz, ^4J = 1.2 Hz, ArH), 7.88 (m, 1H, ArH), 7.97 (m, 1H, ArH), 8.02 (dd, 1H, ^3J = 8.5 Hz, ^4J = 1.2 Hz, ArH), 8.40 (d, 1H, ^3J = 7.6 Hz, ArH), 8.59 (d, 1 H, ^3J = 7.6 Hz, ArH), 8.63 (dd, 1H, ^3J = 7.3 Hz, ^4J = 0.9 Hz), 8.81 (dd, 1H, ^3J = 8.5 Hz, ^4J = 0.9 Hz).

5.9. Synthesis of 1–5 and 7

1,8-Naphthalic anhydrides were suspended in 15 mL EtOH abs and an excess of amine was added. The mixture was stirred under reflux conditions for 5–7.5 h. After evaporation of the solvent, the naphthalimides were isolated by column chromatography (CC) over SiO_2. Some compounds were obtained as hydrates (the presence of water was confirmed by ^{1}H NMR in $CDCl_3$) due to water impurities in the chromatographic solvents.

5.10. *N*-(*N*′,*N*′-Dimethyl-2-aminoethyl)-4-ethylthio-1,8-naphthalimide (1)

4-Ethylthio-1,8-naphthalic anhydride: 106 mg, (0.41 mmol), 0.15 mL *N*,*N*-dimethylethylamine; 5 h, CC: $CHCl_3$ followed by ethylacetate/methanol 9:1 and 8:2; yield: 128 mg (0.39 mmol, 95%) yellow crystals (mp 103 °C); ^{1}H NMR ($CDCL_3$): δ = 1.50 (t, 3 H, ^3J = 7.6 Hz), 2.39 (s, 6H, N(CH_3)$_2$), 2.68 (t, 2H, ^3J = 7.2 Hz), 3.21 (q, 2H, ^3J = 7.6 Hz), 4.34 (t, 2H, ^3J = 7.2 Hz), 7.56 (d, 1H, ^3J = 8.0 Hz, ArH), 7.76 (m, 1H, ArH), 8.49 (d, 1H, ^3J = 8.0 Hz, ArH), 8.58 (m, 1H, ArH), 8.64 (m, 1H, ArH); MS (EI): *m*/*z* = 328 (2.1%, M^+), 298 (0.3%, M^+-2 CH_3), 58 (100%). Anal. (Calcd/Found): C (65.83/65.70), H (6.14/6.14), N (8.53/8.53).

5.11. *N*-(*N*′,*N*′-Dimethyl-2-aminoethyl)-4-butylthio-1,8-naphthalimide (2)

4-Butylthio-1,8-naphthalic anhydride: 104 mg (0.36 mmol), 0.2 mL *N*,*N*-dimethylaminoethylamine; 6.5 h, CC: ethylacetate/methanol 4:1 and CH_2Cl_2, CH_2Cl_2/MeOH 5:1; yield: 72 mg (0.20 mmol, 56%) yellow crystals; ^{1}H NMR ($CDCl_3$): δ = 0.99 (t, 3H, ^3J = 7.3 Hz, –CH_3), 1.56 (m, 2H, CH_2), 1.80 (m, 2H, CH_2), 2.36 (s, 6H, –N(CH_3)$_2$), 2.66 (t, 2H, ^3J = 7.1 Hz, CH_2), 3.16 (t, 2H, ^3J = 7.4 Hz, CH_2), 4.32 (t, 2H, ^3J = 7.1 Hz, CH_2), 7.54 (d, 1H, ^3J = 7.9 Hz, ArH), 7.74 (dd, 1H, ^3J = 8.5 Hz, ^3J = 7.3 Hz, ArH), 8.47 (d, 1H, ^3J = 7.9 Hz), 8.58 (dd, 1H, ^3J = 8.5 Hz, ^4J = 1.1 Hz, ArH), 8.62 (dd, 1H, ^3J = 7.3 Hz, ^4J = 1.1 Hz). Anal (Calcd/Found): C (67.38/67.43), H (6.79/6.81), N (7.86/7.77).

5.12. 4-Benzylthio-*N*-(*N*′,*N*′-dimethyl-2-aminoethyl)-1,8-naphthalimide·4H_2O (3)

4-Benzylthio-1,8-naphthalic anhydride: 118 mg (0.37 mmol), 0.20 mL *N*,*N*-dimethylaminoethylamine; 6.5 h, CC: ethylacetate/methanol 4:1 and CH_2Cl_2/methanol 5:1; yield: 88 mg (0.19 mmol, 51%), yellow crystals (mp 252 °C); ^{1}H NMR (DMSO-d_6): δ = 2.82 (br, 2H, CH_2), 3.36 (s, 6H, –N(CH_3)$_2$), 4.22 (t_{br}, 2H, CH_2), 4.57 (s, 2H, CH_2), 7.30 (m, 3H, 3× ArH), 7.49 (m, 2H, 2× ArH), 7.88 (m, 2H, 2× ArH), 8.37 (d, 1H, ^3J = 8.0 Hz, ArH), 8.54 (m, 2H, 2× ArH); MS (EI): *m*/*z* = 390 (3%, M^+), 58 (100%). Anal. (Calcd/Found): C (59.72/59.43), H (6.54/6.19), N (6.06/6.05).

5.13. 4-(2-Aminophenyl)-thio-*N*-(*N*′,*N*′-dimethyl-2-aminoethyl)-1,8-naphthalimide·H_2O (4)

4-(2-Aminophenyl)-thio-1,8-naphthalic anhydride: 106 mg (0.33 mmol), 0.20 mL *N*,*N*-dimethylaminoethylamine; 7.5 h; CC: ethylacetate/methanol 4:1; yield: 115 mg monohydrate (0.28 mmol, 85%), orange crystals (mp 256 °C); ^{1}H NMR (DMSO-d_6): δ = 2.88 (br, 2H, CH_2), 3.37 (s, 6H, –N(CH_3)$_2$), 4.23 (t, 2H,

^3J = 5.8 Hz), 5.57 (s, 2H, NH_2), 6.70 (m, 1H, ArH), 6.91 (m, 1H, ArH), 7.0 (d, 1H, ^3J = 7.9 Hz, ArH), 7.31 (m, 1H, ArH), 7.40 (m, 1H, ArH), 7.96 (m, 1H, ArH), 8.31 (d, 1H, ^3J = 7.9 Hz, ArH), 8.58 (m, 1H, ArH), 8.71 (m, 1H, ArH); MS (EI): m/z = 391 (4.6%, M^+), 58 (100%). Anal. (Calcd/Found): C (64.53/64.38), H (5.66/5.82), N (10.26/10.16).

5.14. 4-(4,5-Benzo-1,3-thiazol-2-yl)-thio-*N*-(*N*′,*N*′-dimethyl-2-aminoethyl)-1,8-naphthalimide·3H_2O (5)

4-(4,5-Benzo-1,3-thiazol-2-yl)-thio-1,8-naphthalic anhydride: 114 mg (0.31 mmol), 0.20 mL *N*,*N*-dimethylaminoethylamine; 6.5 h; SC: CH_3Cl followed by ethylacetate/methanol 8:2 and 4:1; yield: 88 mg (0.18 mmol, 58%), yellow crystals (mp 248 °C); ^1H NMR ($CDCl_3$): δ = 2.96 (d, 6H, ^3J = 4.8 Hz, $-NH^+(CH_3)_2$), 3.44 (m, 2H, CH_2), 4.62 (m, 2H, CH_2), 7.34 (m, 1H, ArH), 7.47 (m, 1H, ArH), 7.68 (m, 1H, ArH), 7.85 (m, 1H, ArH), 7.95 (m, 1H, ArH), 8.24 (d, 1H, ^3J = 7.6 Hz, ArH), 8.64 (d, 1H, ^3J = 7.6 Hz, ArH), 8.70 (m, 1H, ArH), 8.81 (m, 1H, ArH); MS (EI): m/z = 433 (5.7%, M^+), 58 (100%). Anal. (Calcd/Found): C (56.66/56.99), H (5.17/4.92), N (8.62/8.88).

5.15. *N*-(*N*′,*N*′-Dimethylaminoethyl)-1,8-naphthalimide (7)

1,8-Naphthalic anhydride: 200 mg (1.01 mmol), 0.20 mL *N*,*N*-dimethylaminoethylamine; 6.5 h; CC: dichloromethane/methanol 8:2; yield: 252 mg (0.94 mmol, 94%) white crystals, ^1H NMR ($CDCl_3$): δ = 2.37 (s, 6H, $-N(CH_3)_2$), 2.67 (t, 2H, ^3J = 7.1 Hz CH_2), 4.35 (t, 2H, ^3J = 7.1 Hz CH_2), 7.75 (dd, 2H, ^3J = 7.4 Hz, ^3J = 8.0 Hz, 2× ArH), 8.21 (m, 2H, 2× ArH), 8.61 (dd, 2H, ^3J = 7.4 Hz, ^4J = 0.8 Hz, 2× ArH). Anal. (Calcd/Found): C (71.62/71.84), H (6.01/6.19), N (10.44/10.06); preparation of **7** without NMR structural characterization data has been reported.[2,25]

5.16. Synthesis of 4-ethylthio-*N*-(2-thiolethyl)-1,8-naphthalimide (6)

4-Ethylthio-1,8-naphthalic anhydride (630 mg, 2.44 mmol) was suspended in 50 mL absolute ethanol, 410 mg (3.61 mmol) cysteamine hydrochloride, and 0.5 mL triethylamine were added and the mixture was stirred under reflux condition for 6 h. The formed precipitate was isolated by filtration, washed with ethanol, and dried. Yield 579 mg (1.76 mmol, 72%) yellow crystals; ^1H NMR (DMSO-d_6): δ = 1.37 (t, 3H, ^3J = 7.3 Hz, CH_3), 3.05 (t, 2H, ^3J = 7.2 Hz, CH_2), 3.25 (q, 2H, ^3J = 7.3 Hz, CH_2), 4.33 (t, 2H, ^3J = 7.2 Hz, CH_2), 7.72 (d, 1H, ^3J = 8.0 Hz, ArH), 7.86 (dd, 1H, ^3J = 7.9 Hz, ^3J = 7.9 Hz, ArH), 8.33 (d, 1H, ^3J = 8.0 Hz, ArH), 8.50 (m, 2H, 2× ArH); MS (EI): m/z = 317 (24.6%, M^+), 284 (68.1%, M^+-H_2S), 258 (100%). Anal. (Calcd/Found): C (60.54/60.30), H (4.76/4.75), N (4.41/4.66).

5.17. Fluorescence scans and DNA fluorescence-quenching

Compounds were prepared as 5.0 mM stock solutions in DMSO. For initial fluorescence-scanning investigations, the stock solutions were diluted 1:1000 with PBS and measured. For DNA-binding studies, the stock solutions were diluted 1:1000 with PBS containing DNA in graded concentrations (nucleoside concentration: 0, 5, 25, 50, 100, 200, 400 μM), incubated for 60 min at 37 °C and measured. Fluorescence measurements were performed using a Hitachi F-4500 fluorescence spectrometer.

5.18. DNA binding studies (thermal denaturation, UV/vis, and circular dichroism)

The thermal denaturation temperature T_m of 1:10 compound/DNA mixtures [compound concentration: 20 μM, DNA concentration = M(nucleotide) = 200 μM] were determined in a 10 mM phosphate buffer at pH = 7.2 in the presence of 1% DMSO. Melting curves were recorded at 1 °C steps for the wavelength 260 nm with an Analytik Jena SPECORD 200 spectrometer equipped with a Peltier temperature controller. T_m values were calculated by determining the midpoints of melting curves from the first-order derivatives. The experimental ΔT_m values are estimated to be accurate within ±1 °C. Concentrations of CT DNA were determined spectrophotometrically using the molar extinction coefficient ε_{260} = 6600 M^{-1} cm^{-1}.[42] All electronic absorption measurements were performed at 293 K. After sonication, buffered solutions of CT DNA gave a UV absorbance ratio A_{260}/A_{280} of approximately 1.90, indicating that the DNA was sufficiently free of proton.[43] Twenty micromolar solutions of the compounds were treated with 200 μM DNA (nucleotide) for 60 min. All UV/vis and CD spectra were measured after equilibration, that is, no further change in the monitored absorbance or molar ellipticity. The UV/vis measurements were performed on an Analytik Jena SPECORD 200 spectrometer and the CD measurements on a Jasco J-715 instrument.

5.19. DNA photocleavage

To 0.25 μg covalently closed pBR322 plasmid DNA (Takara Biotechnology, Dalian, China) in 9 μL buffer (Tris–HCl, pH 7.5) 1.0 μL of a 0.5 mM stock solution of **1–7** in DMSO or blank DMSO (control) was added. The solutions were irradiated for 2 h at 365 nm (8 W, distance: 10 cm). Gel electrophoresis of the samples was performed in a 1% agarose gel. DNA was visualized by ethidium bromide staining and photographed. Cleaved DNA was quantified using Gel-Pro Analyzer software (Version 4.0) and expressed as percentage of the total.

5.20. Western blot analysis of Topo IIα level after drugs treatment

HeLa cells (1×10^6/dish) were seeded in 10-cm dishes. After 12 h of incubation, cells were treated with drugs (**1–7**) and R16 at the concentration of their IC_{50} values (as determined in separate experiments, see Supporting information) for 24 h, respectively. Cells were lysed in a 0.1% NP40 buffer containing 10 mM NaCl, 5 mM EDTA, 50 mM NaF, 50 mM Tris–HCl (pH 7.5), 1 mM phenylmethylsulfonyl fluoride, 20 mg/mL leupeptin, 20 mg/mL aprotonin, 20 mg/mL antipaoen, 1 mM DTT, and 0.1% SDS and placed in ice for 30 min. After centrifugation for 15 min at 4 °C, the supernatant was collected. Lysates were quantified using the BCA protein assay (Pierce Biochemicals, Rockland, IL). For Western blot analysis, equal amounts of proteins (50 μg) were separated by SDS–polyacrylamide gel electrophoresis and transferred to a nitrocellulose membrane. The blot was blocked in blocking buffer (5% non-fat dry milk/1% Tween 20 in PBS) for 1 h at room temperature and then incubated overnight with appropriate primary antibodies in blocking buffer overnight at 4 °C. The blot was then incubated with appropriate secondary antibody alkaline phosphatase (AP) conjugate and detected in 10 mL AP buffer containing 33 μL BCIP and 66 μl NBT (at room temperature for 10–20 min), and then photographed. β-Actin was used as a loading control.

5.21. Fluorescence microscopic studies

MCF-7 cells were grown in 6-well plates (Sarstedt) until at least 70% confluence. The cell culture medium was replaced with fresh medium containing the compounds in a concentration of 10 μM (0.1% V/V DMSO) and incubated for 6 h at 37 °C in a 5% CO_2/95% air atmosphere. The medium was removed, the cells were washed with PBS, and finally 500 μL PBS was added to each well. Fluorescence microscopy was performed using a Axiovert 40 CFL micro-

scope (Zeiss) equipped with a 50 W mercury vapor short arc lamp and a E_x/E_m $390^{\pm 11}/460^{\pm 25}$ nm filter.

5.22. Antiproliferative effects and phototoxicity

The continuous exposure experiments were performed according to a previously described assay procedure.[38] In short each 100 μL of 10,000 cells/mL (MCF-7) or 2850 cells/mL (HT-29) were incubated in 96-well plates at 37 °C in 5% CO_2/95% air atmosphere for 48 h (HT-29) or 72 h (MCF-7). Then the medium was replaced with medium containing the drugs in graded concentrations (200 μL per well, six replicates). After further incubation for 72 h (HT-29) or 96 h (MCF-7), the cell biomass was determined by crystal violet staining. For the short-time incubation and phototoxicity experiments this procedure was modified as follows: after 24 h of incubation with the drug containing media, the wells were emptied and new drug-free cell culture medium was added (200 μL per well). The plates for evaluation of phototoxic effects were placed under a 4 W UV lamp and irradiated at 366 nm for 20 min at a distance of 5 cm. Then incubation at 37 °C in 5% CO_2/95% air atmosphere was continued for further 48 h (HT-29) or 72 h (MCF-7). The cell biomasses were determined by crystal violet staining. IC_{50} values were determined as that concentration causing 50% inhibition of cell proliferation compared to an untreated control and expressed as mean value of at least two independent experiments.

Acknowledgment

Dr. Ingo Ott appreciates a postdoctoral fellowship from East China University of Science and Technology.

Supplementary data

The supporting information contains results from the DNA interaction studies (UV/vis spectra), cytotoxicity experiments against Hela cells and evaluation of the cell growth characteristics of HT-29 and MCF-7 cells. This information is available free of charge in the internet. Supplementary data associated with this article can be found, on the online version, at doi:10.1016/j.bmc.2008.06.052.

References

1. Brana, M. F.; Ramos, A. *Curr. Med. Chem. Anti-Cancer Agents* **2001**, *1*, 237.
2. Idoipe, A.; Santillan, M. S.; Martinez-Larranaga, M. R.; Gonzalez, E.; de Jalon, P. D. G. *Arch. Farmacol. Toxicol.* **1979**, *5*, 17.
3. Brana, M. F.; Castellano, J. M.; Jimenez, A. *Cancer Chemother. Pharmacol.* **1980**, *4*, 61.
4. Zee-Cheng, R. K.; Cheng, C. C. *J. Med. Chem.* **1985**, *28*, 1216.
5. Sami, S. M.; Dorr, R. T.; Alberts, D. S.; Solyom, A. M.; Remers, W. A. *J. Med. Chem.* **2000**, *43*, 3067.
6. Brana, M. F.; Cacho, M.; Ramos, A.; Dominguez, M. T.; Pozuelo, J. M.; Abradelo, C.; Rey-Stolle, M. F.; Yuste, M.; Carrasco, C.; Bailly, C. *Org. Biomol. Chem.* **2003**, *1*, 648.
7. Brana, M. F.; Cacho, M.; Garcia, M. A.; de Pascul-Teresa, B.; Ramos, A.; Dominguez, M. T.; Pozuelo, J. M.; Abradelo, C.; Rey-Stolle, M. F.; Yuste, M.; Banez-Coronel, M.; Lacal, J. C. *J. Med. Chem.* **2004**, *47*, 1391.
8. Antonini, I.; Santoni, G.; Lucciarini, R.; Amantini, C.; Sparapani, S.; Magnano, A. *J. Med. Chem.* **2006**, *49*, 7198.
9. Quaquebeke, E. V.; Mahieu, T.; Dumont, P.; Dewelle, J.; Ribaucour, F.; Simon, G.; Sauvage, S.; Gaussin, J. F.; Tuti, J.; El Yazidi, M.; Van Vynckt, F.; Mijatovic, T.; Lefranc, F.; Darro, F.; Kiss, R. *J. Med. Chem.* **2007**, *50*, 4122.
10. Li, Z.; Yang, Q.; Qian, X. *Bioorg. Med. Chem. Lett.* **2005**, *15*, 3143.
11. Li, Z.; Yang, Q.; Qian, X. *Bioorg. Med. Chem.* **2005**, *13*, 4864.
12. Li, F.; Cui, J.; Guo, L.; Qian, X.; Ren, W.; Wang, K.; Liu, F. *Bioorg. Med. Chem.* **2007**, *15*, 5114.
13. Zhu, H.; Huang, M.; Yang, F.; Chen, Y.; Miao, Z. H.; Qian, X.; Xu, Y.; Qin, Y.; Luo, H.; Shen, X.; Geng, M.; Cai, Y.; Ding, J. *Mol. Cancer Ther.* **2007**, *6*, 484.
14. Pardo, A.; Poyato, J. M. L.; Martin, E. *J. Photochem.* **1987**, *36*, 323.
15. Cao, H.; Chang, V.; Hernandez, R.; Heagy, M. D. *J. Org. Chem.* **2005**, *70*, 4929.
16. Qian, X.; Li, Y.; Xu, Y.; Liu, Y.; Qu, B. *Bioorg. Med. Chem. Lett.* **2004**, *14*, 2665–2668.
17. Li, Z.; Yang, Q.; Qian, X. *Bioorg. Med. Chem. Lett.* **2005**, *15*, 1769.
18. Xu, Y.; Qu, B.; Qian, X.; Li, Y. *Bioorg. Med. Chem. Lett.* **2005**, *15*, 1139.
19. Yang, Q.; Qian, X.; Xu, J.; Sun, Y.; Li, Y. *Bioorg. Med. Chem.* **2005**, *13*, 1615.
20. Rogers, J. E.; Abraham, B.; Rostkowski, A.; Kelly, L. A. *Photochem. Photobiol.* **2001**, *74*, 521.
21. Chanh, T. C.; Lewis, D. E.; Allan, J. S.; Sogandares-Bernal, F.; Judy, M. M.; Utecht, R. E.; Matthews, J. L. *AIDS Res. Hum. Retroviruses* **1993**, *9*, 891.
22. Chanh, T. C.; Lewis, D. E.; Judy, M. M.; Sogandares-Bernal, F.; Michalek, G. R.; Utecht, R. E.; Skiles, H.; Chang, S. C.; Matthews, J. L. *Antiviral Res.* **1994**, *25*, 133.
23. Pervaiz, S. *FASEB J.* **2001**, *15*, 612.
24. Qian, X.; Huang, T. B.; Wei, D. Z.; Zhu, D. H.; Fan, M. C.; Yao, W. *J. Chem. Soc. Perkin. Trans. 2* **2000**, 715–718.
25. Ramachandram, B.; Saroja, G.; Sankaran, N. B.; Samanta, A. *J. Phys. Chem. B* **2000**, *104*, 11824.
26. Ramachandram, B. *J. Fluoresc.* **2005**, *15*, 71.
27. Cho, D. W.; Fujitsuka, M.; Sugimoto, A.; Yoon, U. C.; Mariano, P. S.; Majima, T. *J. Phys. Chem. B* **2006**, *110*, 11062.
28. Schäfer, S.; Ott, I.; Gust, R.; Sheldrick, W. S. *Eur. J. Inorg. Chem.* **2007**, 3034.
29. Grabchev, I.; Chovelon, J. M.; Qian, X. *J. Photochem. Photobiol. A* **2003**, *158*, 37.
30. Xu, Z.; Qian, X.; Cui, J. *Org. Lett.* **2005**, *7*, 3029.
31. Zhang, Z.; Wu, D.; Guo, X.; Qian, X.; Lu, Z.; Xu, Q.; Yang, Y.; Duan, L.; He, Y.; Feng, Z. *Chem. Res. Toxicol.* **2005**, *18*, 1814.
32. Xu, Z.; Xiao, Y.; Qian, X.; Cui, J.; Cui, D. *Org. Lett.* **2005**, *7*, 889.
33. Parkesh, R.; Lee, T. C.; Gunssnlaugson, T. *Org. Biomol. Chem.* **2007**, *5*, 310.
34. Cui, D.; Qian, X.; Liu, F.; Zhang, R. *Org. Lett.* **2004**, *6*, 2757.
35. Martin, E.; Weigand, R.; Pardo, R. *J. Lumin.* **1996**, *68*, 157.
36. Berque-Bestel, I.; Soulier, J. L.; Giner, M.; Rivail, L.; Langlois, M.; Sicsic, S. *J. Med. Chem.* **2003**, *46*, 2606.
37. Vazquez, M. E.; Blanco, J. B.; Imperiali, B. *J. Am. Chem. Soc.* **2005**, *127*, 1300.
38. Ott, I.; Schmidt, K.; Kircher, B.; Schumacher, P.; Wiglenda, T.; Gust, R. *J. Med. Chem.* **2005**, *48*, 622.
39. Vazquez, M. E.; Blanco, J. B.; Salvadori, S.; Trapella, C.; Argazzi, R.; Bryant, S. D.; Jinsmaa, Y.; Lazarus, L. H.; Negri, L.; Giannini, E.; Lattanzi, R.; Colucci, M.; Balboni, G. *J. Med. Chem.* **2006**, *49*, 3653.
40. Muller, P. J.; Wilson, B. C. *Lasers Surg. Med.* **2006**, *38*, 384.
41. Dougherty, T. J.; Gomer, C. J.; Henderson, B. W.; Jori, G.; Kessel, D.; Korbelik, M.; Moan, J.; Peng, Q. *J. Nat. Cancer Inst.* **1998**, *90*, 889.
42. Liu, H. Q.; Cheung, T. C.; Peng, S. M.; Chi, M. C. *J. Chem. Soc., Chem. Commun.* **1995**, 1787.
43. Marmur, J. *J. Mol. Biol.* **1961**, *3*, 208.